Consequences of the minimum energy principle for the cutting process

CONSEQUENCES OF THE MINIMUM ENERGY PRINCIPLE FOR THE CUTTING PROCESS.

By J.H. Dautzenberg and A.C.H. van der Wolf

Eindhoven University Press
WPT-Report nr. 0526

Note for STC "C", subgroup "Fundamentals"
Paris, January, 1982.

1. Introduction.

In the past, several researchers made a plasticity model of the cutting process. For all these models, the correspondence between theory and experiment was moderate. For this reason we made a new model [2] in which we assumed the cutting process to be a plastic one. This plastic process occurs in one shear plane in the primary shear zone and also in the secondary shear zone. This secondary shear zone is the chip-tool contact zone. In our view it means that friction in the secondary shear zone origins also from a plastic process. We also assumed that the frictional force depends upon the shear angle. This assumption differs from the known models and is essential for the solution. For both deformation zones we can calculate the necessary power as a function of the shear angle (Section 2). We can find a differential equation using the principle [2] that the best solution of the permitted geometries (determined by the shear angle) is found for the minimum difference between the calculated and measured cutting power. This equation describes the dependence of the first derivative of the normalized frictional force with respect to the shear angle as a function of the normalized frictional force, the shear angle, the rake angle of the tool and the strainhardening exponent of the workpiece material. This normalized frictional force is defined as the frictional force on the tool divided by the specific stress of the workpiece material, the feed and the width of cut. This differential equation, combined with a boundary condition derived from the upsetting test, can be numerically solved. The solution - the normalized frictional force as a function of the shear angle for a given workpiece material characterized by the strainhardening exponent and rake angle of the tool - has been tested by experiments [1]. Comparison of the theoretical and experimental results shows some scatter. In order ro obtain more information about the validity of the proposed model, we ought to compare theoretical and experimental data, not from the solution of the differential equation, but from the differential equation itself. This comparison is carried out for two workpiece materials, different tool materials, feeds, cutting speeds and two rake angles of the tool (Section 3). In the discussion (Section 4) we deal with some explanations for the difference between the experimental and theoretical data.

CONSEQUENCES OF THE MINIMUM ENERGY PRINCIPLE FOR THE CUTTING PROCESS

J.H. Dautzenberg and A.C.H. van der Wolf.
(Division of Production Technology, University of Technology, Eindhoven The Netherlands).

Summary.

Starting with the idea that the cutting process is a plastic process,we have derived a differential equation using the minimum energy principle [1]. This equation shows a relation between the first derivative of the normalized frictional force, the normalized frictional force, the shear angle and the rake angle of the tool. In this equation the properties of the workpiece material are described by the two plastic material constants: the specific stress and the strain hardening exponent. This differential equation confronted with a boundary condition derived from the upsetting test, has been integrated numerically. This yields the relation between the normalized frictional force and the shear angle. In testing this dependence we found the experimental data scattering around the theoretically predicted curves. In order to explain this behaviour, more information about the differential equation itself is needed. Consequently, we determine this equation numerically and compare the results with the experimental data. The cutting tests are performed with two workpiece materials, several tool materials and under different cutting conditions.

2. A cutting model.

We will start with the idea that cutting is a plastic deformation process [1]. The process takes place in 2 regions: the primary shear zone and the secondary shear zone (Figure 1). If we assume that the deformation in the primary shear zone takes place in only one plane, it holds for the power:

$$E_p = \frac{C}{n+1} \left\{ \frac{\text{cotan } \varphi + \tan (\varphi - \gamma_o)}{\sqrt{3}} \right\}^{n+1} bfv \qquad (1)$$

with: v = cutting speed,
b = width of cut,
f = feed,
C = specific stress of the workpiece material,
φ = shear angle in the primary shear zone,
γ_o = rake angle of the tool,
n = strain hardening exponent of the workpiece material.

For the power in the secondary shear zone it holds:

$$E_s = \frac{Fv \sin \varphi}{\cos (\varphi - \gamma_o)} \qquad (2)$$

with F = frictional force on the chip.

This quantity F is defined by:

$$F = - F_w = - \{F_v \sin \gamma_o + F_f \cos \gamma_o\} \qquad (3)$$

where F_f is the feed force, F_v is the cutting force on the tool and F_w is the frictional force on the tool.

The best solution for the class of geometries in which only the shear angle can vary, is determined by:

$$\frac{d (E_s + E_p)}{d\varphi} = 0 \qquad (4)$$

This means that the difference between the measured cutting power and the power calculated for the chosen geometry is minimal. Also it is proven that for this geometry the calculated power function has a minimum.

φ = shear angle
γ_o = rake angle of the tool
v = cutting speed
v_c = chip speed
f = feed
h_c = chip thickness
F_f = feed force
F_v = cutting force

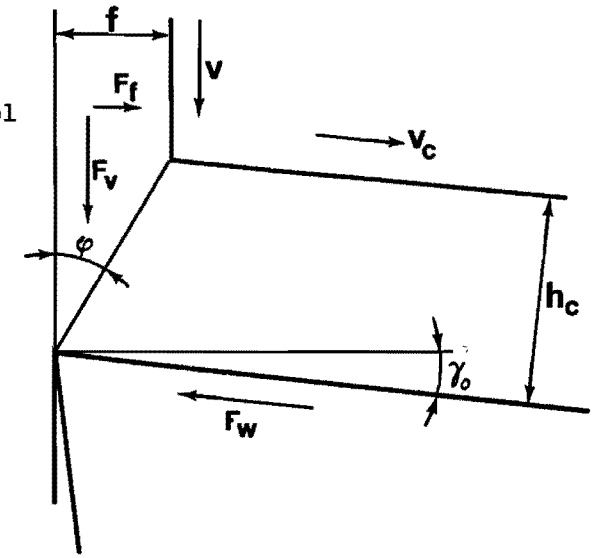

Figure 1. Schematic representation of the cutting process in two dimensions.

Taking into account the variation of F as a function of the shear angle φ and combining Eq. (1), (2) and (4) it holds after some calculations:

$$\frac{1}{Cbf}\frac{dF}{d\varphi} = -\frac{F\cos\gamma_o}{Cbf\cos(\varphi-\gamma_o)\sin\varphi} + \frac{\cos(\varphi-\gamma_o)}{\sqrt{3}\sin\varphi} \ast$$

$$\ast \left\{\frac{\text{cotan}\,\varphi + \tan(\varphi-\gamma_o)}{\sqrt{3}}\right\}^n \left\{\frac{1}{\sin^2\varphi} - \frac{1}{\cos^2(\varphi-\gamma_o)}\right\} \qquad (5)$$

It means that the first derivative of the normalized frictional force $<< = \frac{1}{Cbf} \cdot \frac{dF}{d\varphi} >>$ is a function of the normalized frictional force $<< = \frac{F}{Cbf} >>$, the shear angle φ, the strain hardening exponent n and the rake angle of the tool γ_o. For each workpiece material described by the material constants C and n, Eq. (5) has to be valid for every tool material, feed, width of cut and cutting speed. The problems are the determination of C under the cutting conditions in the primary shear zone and the boundary condition for Eq. (5). This boundary condition can be derived from the upsetting test. In this test the deformation starts in a plane which is inclined 45^o with respect to the upsetting force (Figure 2). Assuming that the location of the first deformation in the beginning of both processes is the same, it holds:

$$F_w = \left|\frac{\tau_{shi}\, bf}{\sin^2 45}\sin\gamma_o\right| \qquad (6)$$

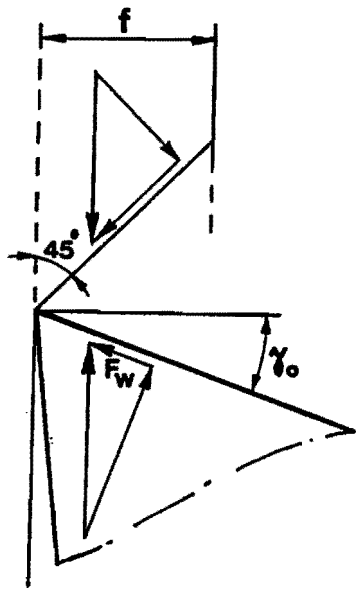

Figure 2. The initiation of the deformation process in cutting.

In Eq. (6) τ_{shi} is the flow stress of the workpiece material. For an ideal plastic material Eq. (6) results in:

$$\frac{F_w}{Cbf} = \left|\frac{\sin \gamma_o}{\sqrt{3}\ \sin^2 45^o}\right| \tag{7}$$

For the determination of the specific stress C we proceed from Figure 1. In this figure the average shear stress $\tau_{shi\ med}$ in the shear plane is:

$$\tau_{shi\ med} = \frac{\sqrt{F_v^2 + F_f^2}\ \cos(\varphi+\beta)\ \sin\varphi}{fb} \tag{8}$$

with $\beta = \arctan\left(\frac{F_f}{F_v}\right)$ (9)

If the shear velocity in the shear plane is constant and the stress-strain behaviour of the workpiece material is described by the Nadai relation, it holds for C using Eq. (8) [1]:

$$C = \frac{\sqrt{F_v^2 + F_f^2}\ \cos(\varphi+\beta)\ \sin\varphi\ (n+1)\ \sqrt{3}}{fb} \left\{\frac{\sqrt{3}}{\operatorname{cotan}\varphi + \tan(\varphi-\gamma_o)}\right\}^{-n} \tag{10}$$

In [1] we have compared the numerically integrated form of Eq. (5) with experimental results. For this numerical integration we used the boundary condition defined by Eq. (7) and the specific stress by Ec. (9)

and (10). The experimental results were optained from two workpiece materials, two different rake angles of the tool, five toolmaterials, one width of cut, several feeds and cutting speeds. The present work contains information about Eq. (5) in a non integrated form.

3. Results.

One of the most important assumptions for the actual model is the dependence of the normalized frictional force on the shear angle. Amongst others, this assumption led to the differential equation represented in Eq. (5). This equation is shown theoretically as well as experimentally in the Figures 3 - 11. In all these figures the theoretical results are represented by curves and the experimental results by symbols. The theoretical curves can be distinguished in two types of curves. They are denoted by A and B. A is the first derivative of the frictional force with respect to the shear angle as a function of the shear angle. This represents both terms of the right side of Eq. (5). Curve B represents the first term on the right side of Eq. (5). Both terms are derived from the numerical integration of Eq. (5) in combination with Eq. (7). The strain hardening exponent is determined in the tensile test in the usual way.
The experimental results [3], [4] denoted by symbols are calculated with Eq. (5). In this calculation, besides the measured quantity F_w with Eq. (3) and the strain hardening exponent, also the values of the specific stress C and the shear angle φ are used. The specific stress is determined by Eq. (10). The shear angle can be derived from the geometry of the process. It holds:

$$\varphi = \arctan \left\{ \frac{\cos \gamma_o}{\frac{h_c}{f} - \sin \gamma_o} \right\} \qquad (11)$$

with h_c = chip thickness.

Figure 3 shows the theoretical curves A and B for a rake angle of the tool of 6^o. A and B represent two curves. The lower curves of A and B have a strainhardening exponent of 0.0; the higher curves one of 0.4. These curves illustrate that a small variation of the strainhardening exponent does not visibly change the positions of curves A and B. Figures 4 and 5 show the response of the workpiece materials C45 and X38CrMo5 on the variation of feed. Both figures show a good agreement between curves and experimental results, in particular for high values of the shear angle. The agreement is less for small values of the shear

angle. From these figures we can conclude that small values of the shear angle nearly always belong to small feeds.
Figures 6 and 7 relate to the behaviour of the workpiece material C45 and X38CrMo5 for different cutting speeds. Again, the agreement between the theoretical and experimental results is good for great values of the shear angle and moderate for small values.
Figures 8 and 9 show the correspondence between the theoretical and experimental results of the workpiece materials C56 and X38CrMo5 for different tool materials. Also in this case the agreement is good for large values and less for small values of the shear angle.
Figure 10 gives a comparison between theoretical and experimental results for the two workpiece materials C45 and X38CrMo5. As already shown in figure 3 and as can be deduced from Eq. (5), this figure proves that the difference in experimental results between the two workpiece materials is not visible because of the small difference of the strainhardening exponent (C45 n = 0.236; X38CrMo5 n = 0.200). Again, the accordance between theory and experiment is good for high values of the shear angle.
Figure 11 shows the behaviour of the workpiece material C45 for two different rake angles (-6°, $+6^{\circ}$) of the tool. As can be derived from Eq. (5), the thoretical curves A and B have to be different for the two rake angles. This difference is also found experimentally. For increasing values of the shear angle φ, the agreement between curves and symbols improves for situation A as well as for situation B.

4. Discussion.

As already mentioned in the introduction we now pay attention to the differential equation itself. This equation,which is represented by Eq. (5) combined with the boundary condition Eq. (7) makes it possible to calculate numerically - for a given strainhardening exponent and rake angle of the tool - the relation between the first derivative of the normalized frictional force with respect to the shear angle as a function of the shear angle. This solution describes the dependence of:
- the cutting conditions: feed and width of cut,
- the plastic properties of the workpiece material: specific stress and strainhardening exponent,
- the geometry of the tool: rake angle,
- the chipreduction ratio and the friction force on the tool.

It also demonstrates that the solution is independent of the tool material and the cutting speed. Consideration of Eq. (5) shows that this relation has two terms. The first term can be verified experimentally. The numerical solution of this term is represented by the curves B in the Figures 3-11. The second term is a pure theoretical one. It is numerically dependent on the shear angle, as is represented by the difference curve between A and B in the Figures 3-11. This claimed behaviour as derived from Eq. (5) and (7) is confirmed experimentally in the Figures 3-11. However, besides this confirmation these figures also show a deviation between the experimental and theoretical results. This deviation seems to increase with a decrease of the shear angle. The comparison of the theoretical and experimental results also shows that the experimental results are always lower than the theoretical curves. In terms of the "minimum energy principle" this means that the power of the cutting process for a given shear angle is in reality lower than as computed for our model. This effect is in agreement with the theory, stating that the power necessary for an assumed deformation field is always higher than the real field. In order to explain this effect more results are necessary; in particular cutting tests which give very small values of the shear angle.

Another possible explanation for the deviation of the experimental and theoretical results may be found in a faulty determination of the shear angle. The shear angle can be calculated with Eq. (11) by measuring the

chip thickness h_c. This measurement is made with a micrometer. Because of the irregular chip surface, the value of h_c cannot be measured exactly but tend to be overestimated. This overestimation leads to a deviation of the shear angle (= $d\varphi$) as determined with Eq(11) by:

$$d\varphi = - \frac{\sin (2\varphi-\gamma_o) + \sin \gamma_o}{2 \cos \gamma_o} \frac{dh_c}{h_c} \qquad (12)$$

$\frac{dh_c}{h_c}$ = relative measuring error of the chip thickness.

From Eq. (12) we can derive that the deviation $d\varphi$ increases with an increase of the shear angle for a constant relative measuring error of the chip thickness. However, this deviation is opposite to the deviation as represented in Figure 4-11. Furthermore we observe that an increase of φ will give a decrease in the first derivative of the normalized frictional force. The combination of the two opposite effects makes it improbable that an eventual measuring error of the chip thickness is responsable for the deviation between the experimental and theoretical results in the figures 4-11. A final decision can be given by measuring the chip thickness in a more accurate way.

In order to produce the experimental results we need the value of the two plastic quantities of the workpiece material: the specific stress and the strainhardening exponent. The strainhardening exponent is derived from tensile tests [1]. The specific stress is not derived from tensile tests but from cutting tests.It is derived from the force balance on the primary shear zone(Eq. (10)).Figure 12 shows the dependence of the specific stress of C45 for different feeds as a function of the cutting speed. From this figure we conclude that an increase of the cutting speed gives an increase of the specific stress. This behaviour is in agreement with the extended Nadai law,which states an increase of flow stress following an increase of deformation rate. Furthermore, we see an increasing specific stress with a decreasing feed. The deviation from the tensile test is most striking for a feed of 0.1 mm/rev. (C from tensile test for C45 = 1170 N/mm^2). We also found the smallest values of the shear angle at low feeds (see Figures 4 and 5). As already stated,the deviation between the calculated and measured first derivative of the normalized frictional force to the shear angle also has a maximum for these shear angles. The dependent behaviour between feed and shear angle means that the specific

power for the cutting process increases with decreasing feed. This behaviour is well known and may be caused by the unsharpness of the cutting edge. In order to clarify this effect more research is necessary.

5. Conclusions.

- The differential equation derived from the proposed cutting model describes the influence of:
  - . the cutting conditions: feed, cutting speed and width of cut,
  - . the plastic properties of the workpiece material: specific stress and strainhardening exponent,
  - . the geometry of the tool: rake angle,
  - . the tool material,
  - . chip thickness,
  - . the friction force on the tool.
- The validity of the differential equation has been proven for two workpiecematerials: C45 and X38CRMo5; five toolmaterials: P20, P40, M40, M20, K10; different cutting speeds: 1-5 m/s; different feeds: 0.10-0.84 mm/rev.; two rake angles of the tool: +6, -6^{o}.
- A further comparison between the theoretical and experimental value of the first derivative of the normalized frictional force with respect to the shear angle as a function of the shear angle shows a difference. This difference is insignificant at high values of the shear angle but increases with decreasing shear angle.
- The deviation between the theoretical and experimental results at low values of the shear angle seems to concentrate at low feeds.
- The specific stress for the cutting test is higher in comparison with the tensile test, as in accordance with the extended Nadai law.
- Much more experimental results are necessary, especially for those workpiece materials, rake angles and cutting conditions which give small values of the shear angle.

Acknowledgements.

The authors are indebted to Mr. A. van Sorgen, Mr. M.Th. de Groot and Ing. W.D.G. Bosma for their experimental assistence and Drs. N.A.L. Touwen for his assistance in processing the experimental results.

References.

1. J.H. Dautzenberg, P.C. Veenstra and A.C.H. van der Wolf:
The minimum energy principle for the cutting process in theory and experiment.
Annals of the CIRP Vol 30/1/1981 p. 1-4.

2. B. Avitzur: Metal Forming: processes and analysis.
McGraw-Hill (1968).

3. A.G. Strous and H. Munnecom: Beitelkrachten bij draaien.
WPT-Rapport nr. 0138. Division of Production Technology, University of Technology Eindhoven, Netherlands (1965).

4. H. Wagtelenberg: HTS afstudeerrapport. Division of Production Technology, University of Technology Eindhoven, Netherlands (1974).

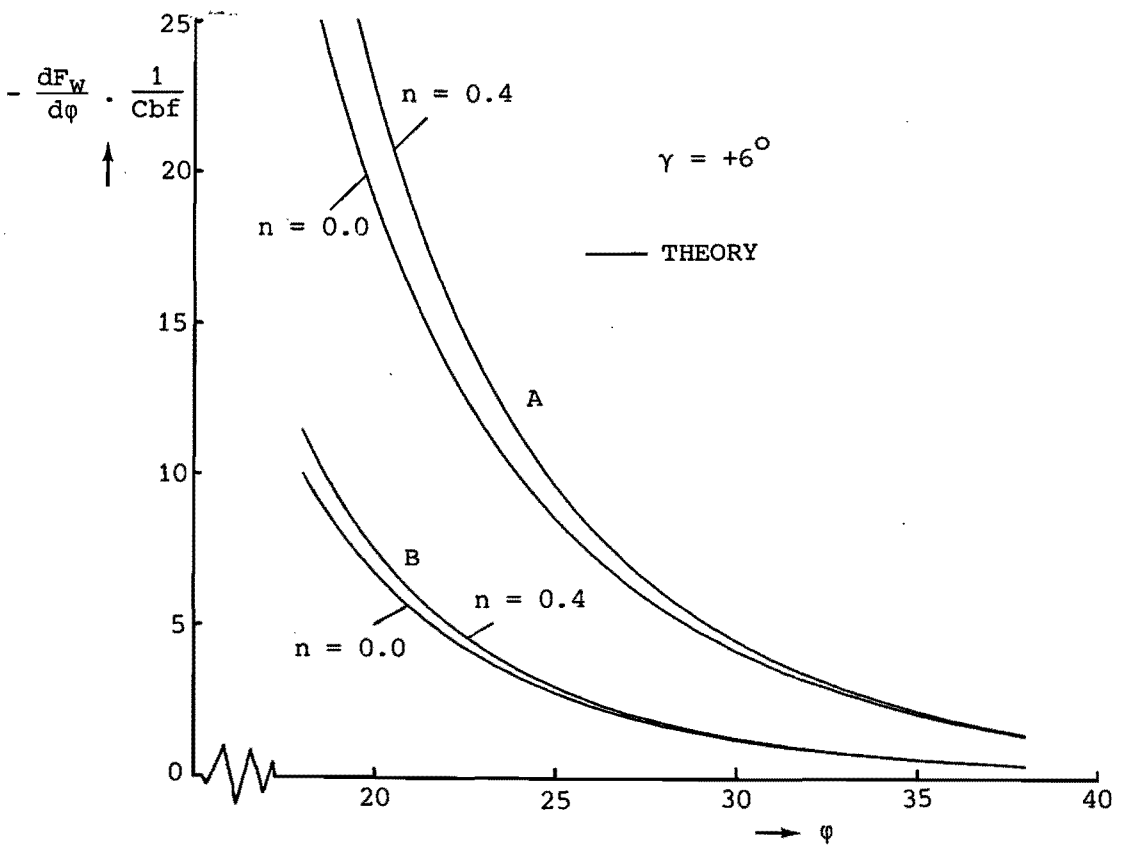

Figure 3: The influence of the strainhardening on the theoretical curves of the first derivative of the normalized frictional force with respect to the shear angle as a function of the shear angle. Curve B is curve A minus the last term of Eq. (5).

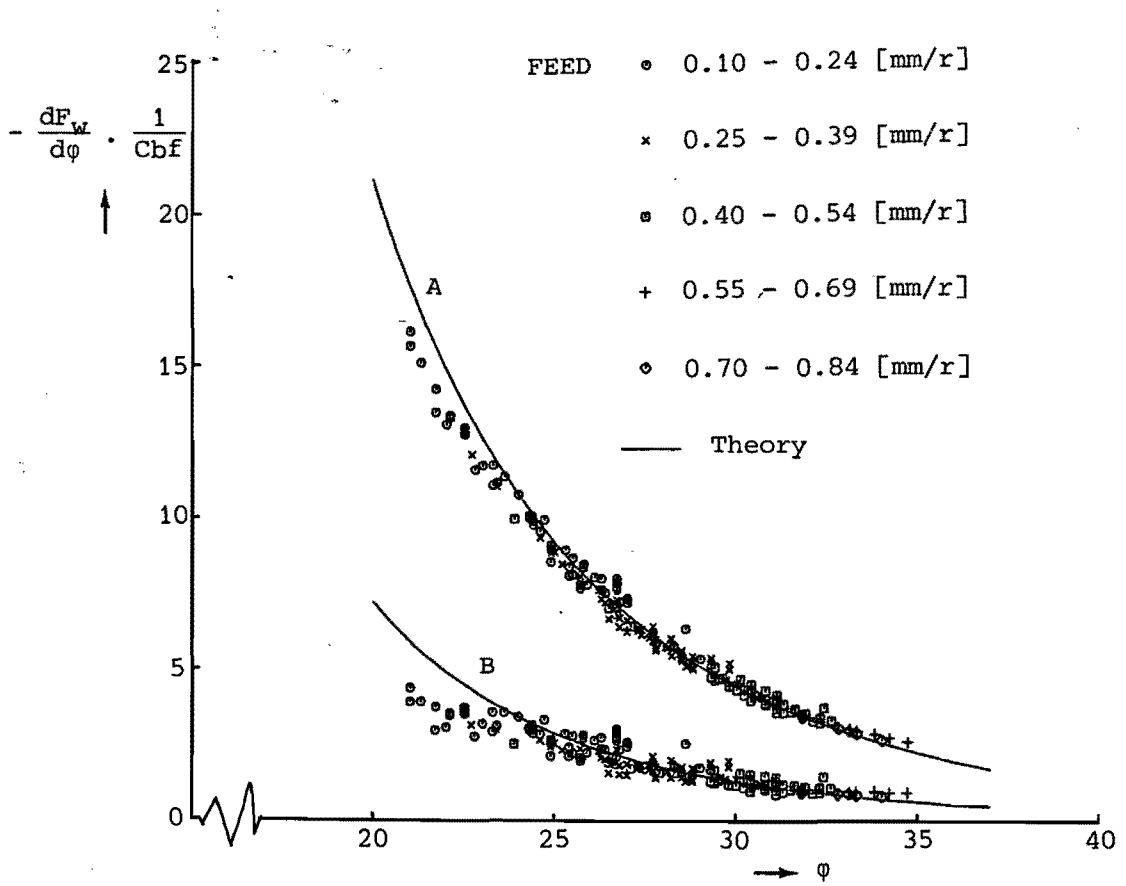

Figure 4: Comparison of theory and experiment for the first derivative of the normalized frictional force with respect to the shear angle as a function of the shear angle for different feeds. Curve B is curve A minus the last term of Eq. (5). Workpiece material C45.

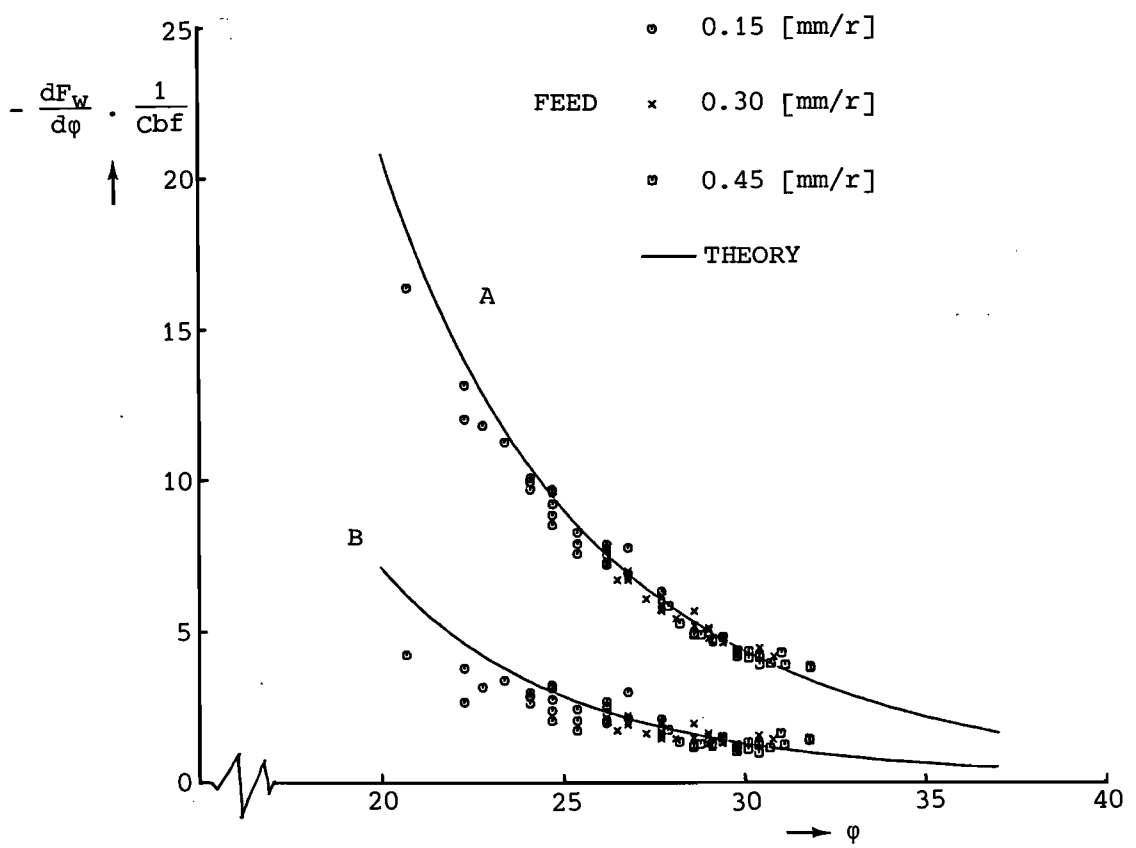

Figure 5: Comparison of theory and experimental for the first derivative of the normalized frictional force with respect to the shear angle as a funtion of the shear angle for different feeds. Curve B is curve A minus the last term of Eq. (5). Workpiece material X38CrMo5.

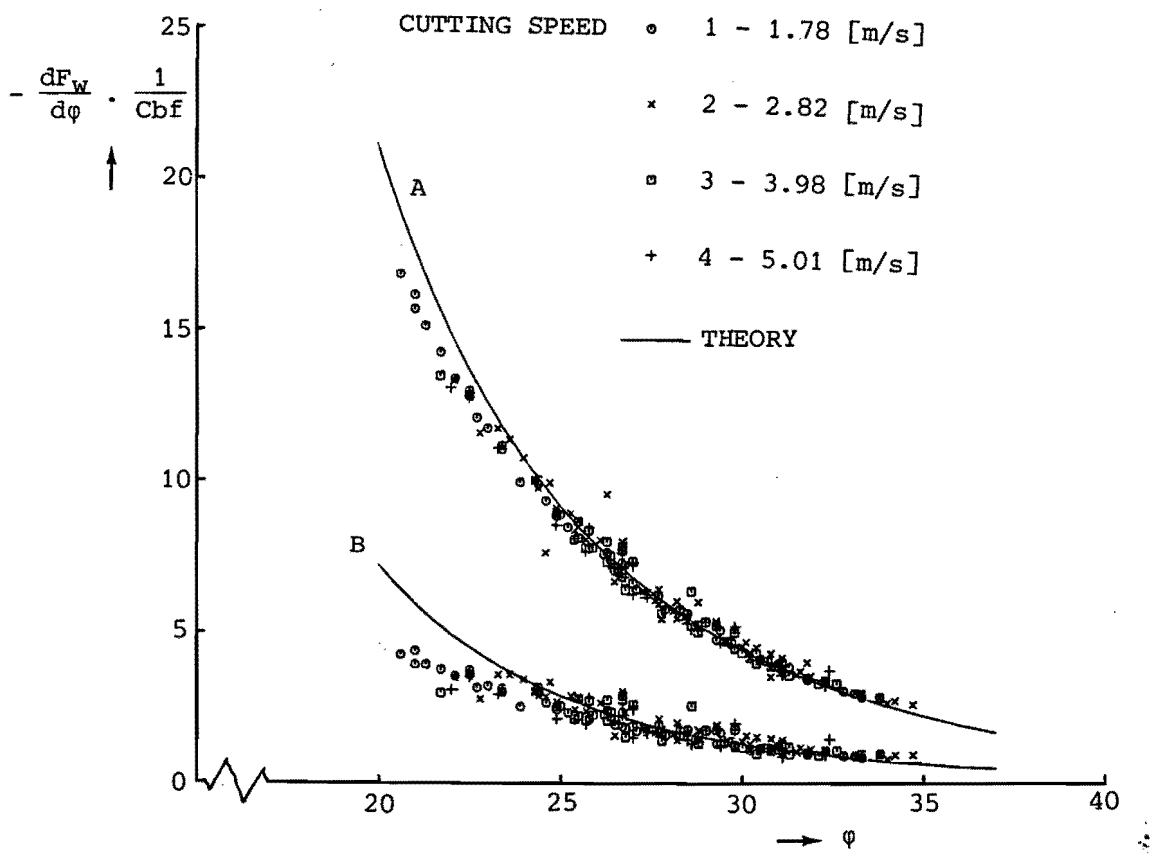

Figure 6: Comparison of theory and experiment for the first derivative of the normalized frictional force with respect to the shear angle as a function of the shear angle for different cutting speeds. Curve B is curve A minus the last term of Eq. (5). Workpiece material C45.

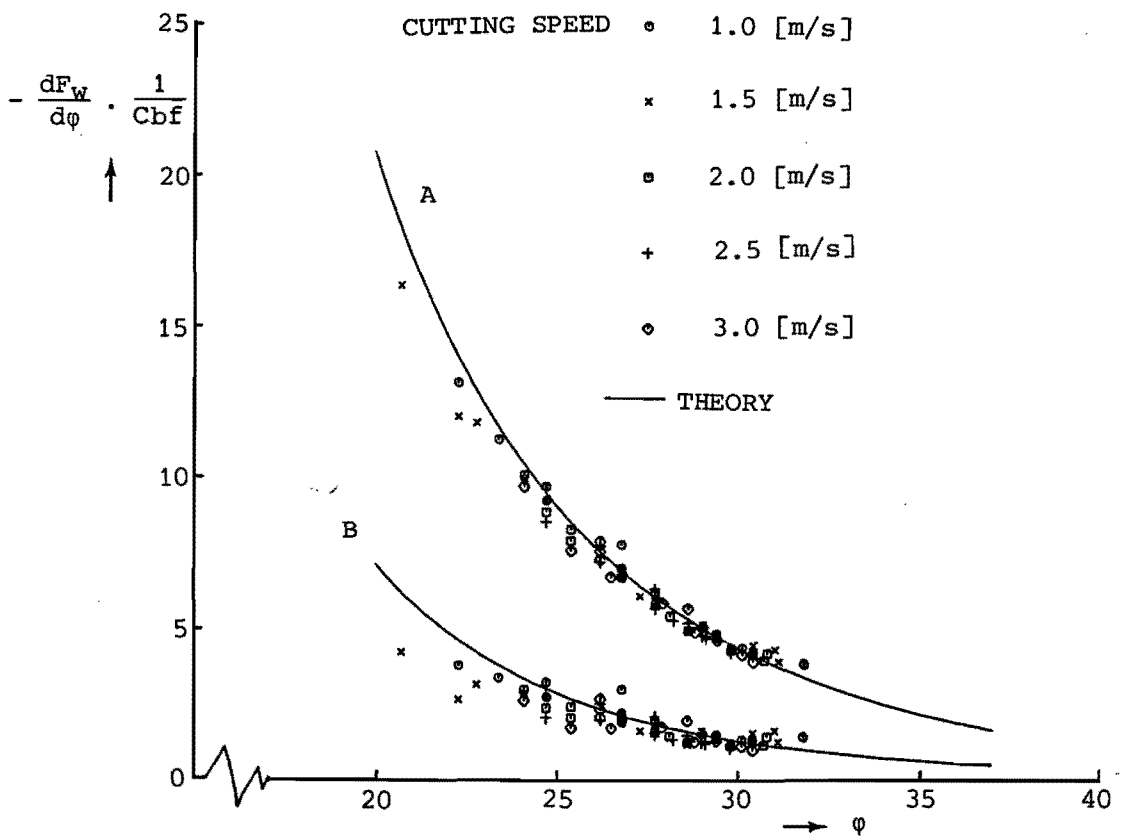

Figure 7: Comparison of theory and experiment for the first derivative of the normalized frictional force with respect to the shear angle as a function of the shear angle for different cutting speeds. Curve B is curve A minus the last term of Eq. (5). Workpiece material X38CrMo5.

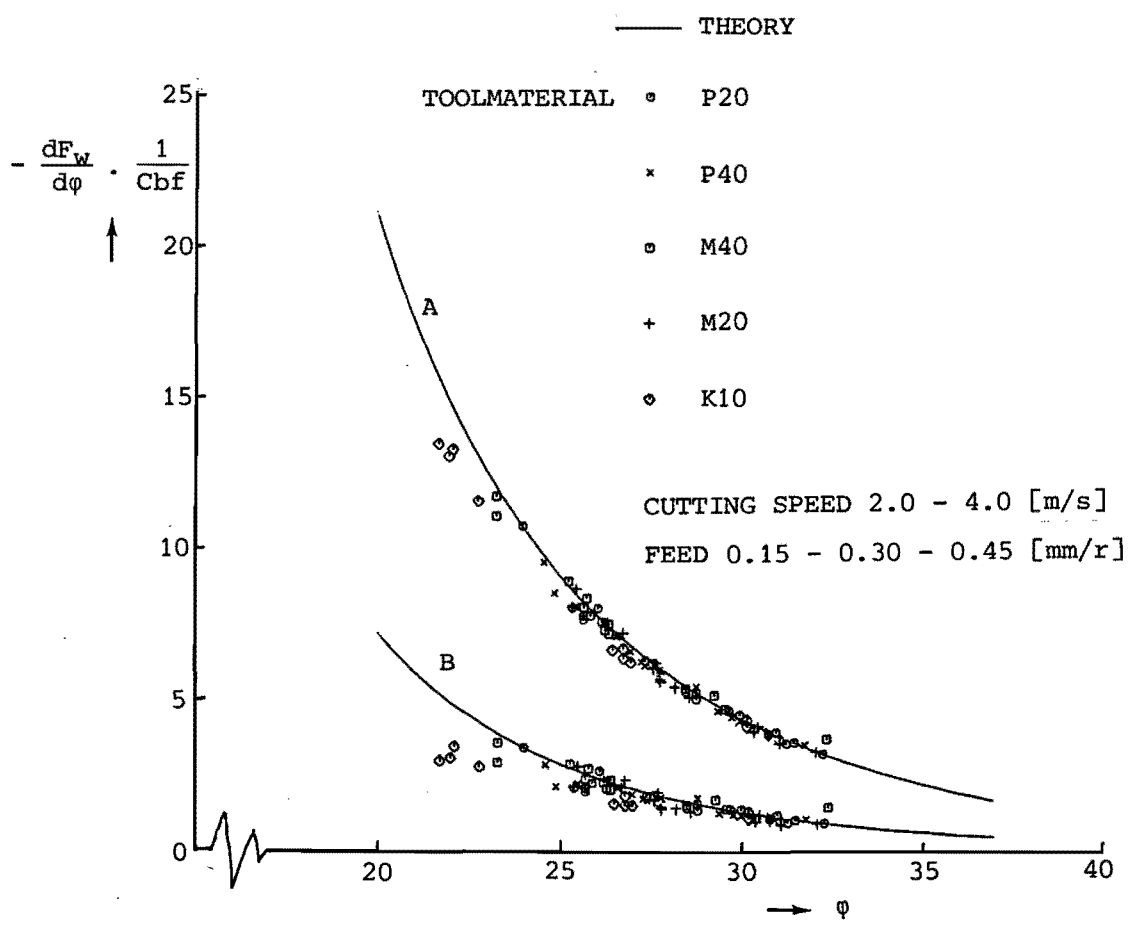

Figure 8: Comparison of theory and experiment for the first derivative of the normalized frictional force with respect to the shear angle as a function of the shear angle for different materials. Curve B is curve A minus the last term of Eg. (5). Workpiece material C45.

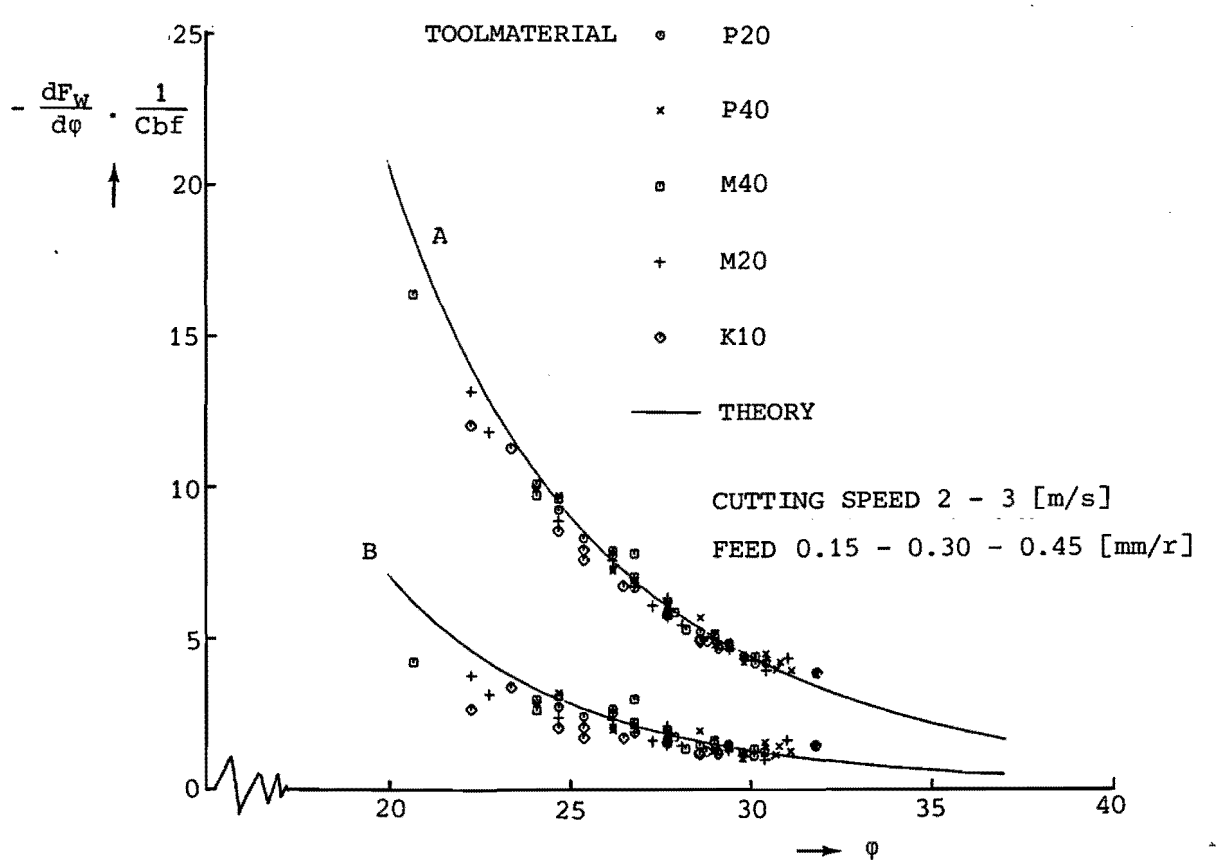

Figure 9: Comparison of theory and experiment for the first derivative of the normalized frictional force with respect to the shear angle as a function of the shear angle for different tool materials. Curve B is curve A minus the last term of Eq. (5). Workpiece material X38CrMo5.

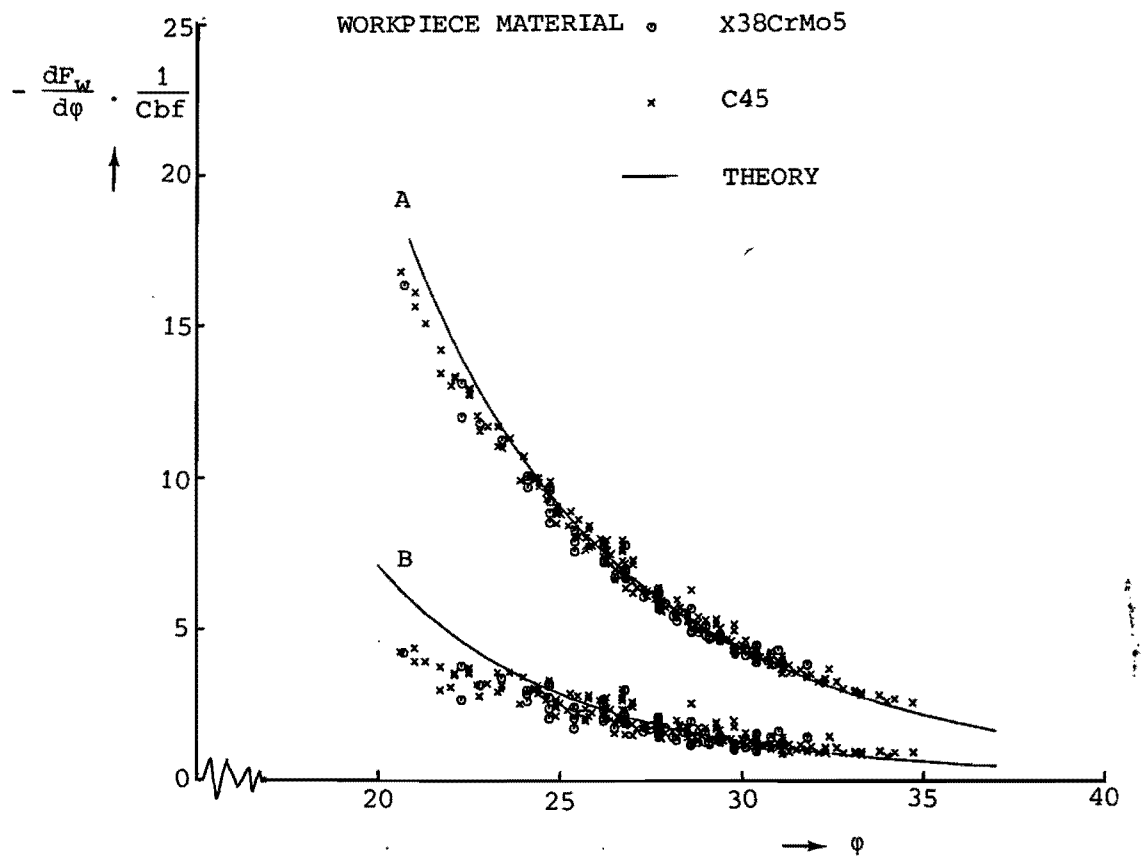

Figure 10: Comparison of theory and experiment for the first derivative of the normalized frictional force with respect to the shear angle as a function of the shear angle for two different workpiece materials. Curve B is curve A minus the last term of Eq. (5).

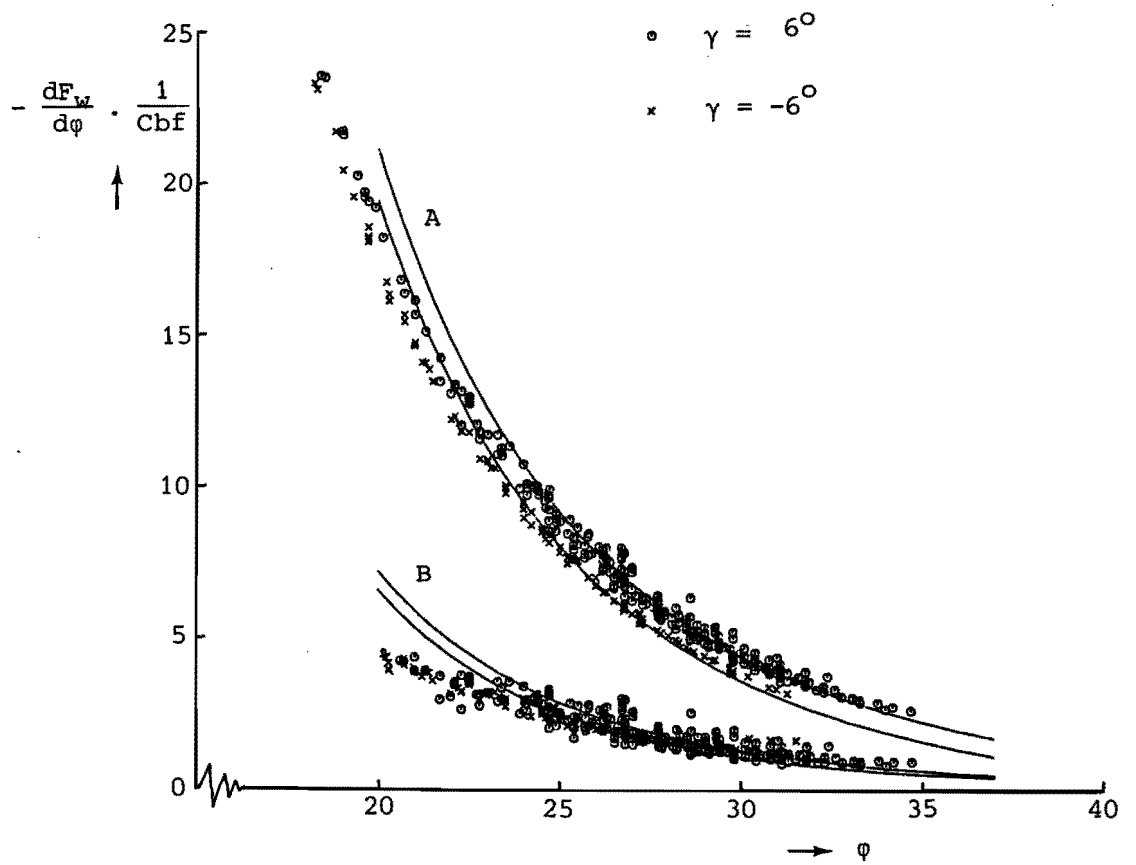

Figure 11: Comparison of theory and experiment for the first derivative of the normalized frictional force with respect to the shear angle as a function of the shear angle for two different rake angles of the tool. Each curve B is the corresponding curve A minus the last term of Eq. (5). Workpiece material C45.

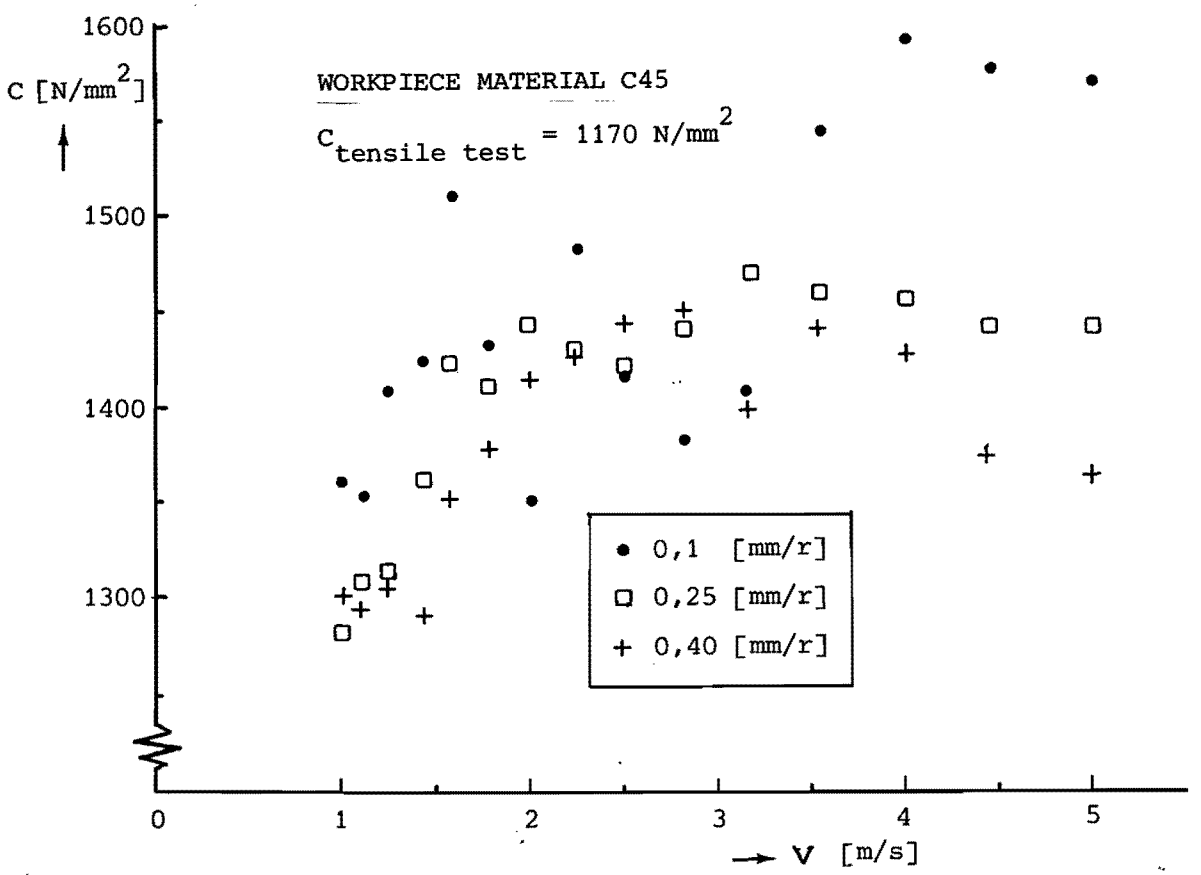

Figure 12: The specific stress of the workpiece material C45 versus the cutting speed, for different feeds.